

Adaptive Super-twisting Sliding Mode Control of Hydraulic Servo Actuator with Nonlinear Features and Modeling Uncertainties

Zhenshuai Wan^{1,2*} – Yu Fu^{1,2} – Longwang Yue¹ – Chong Liu¹

¹ Henan University of Technology, School of Mechanical and Electrical Engineering, China

² Henan University of Technology, Key Laboratory of Grain Information Processing and Control of Ministry of Education, China

This study proposes a novel adaptive super-twisting sliding mode controller (ASTSMC) for hydraulic servo actuator with nonlinear features and modeling uncertainties. In the proposed method, an extended state observer (ESO) is utilized to estimate the value of lumped uncertainties. The core feature of this paper is the combination of ASTSMC with ESO to compensate disturbance in hydraulic servo actuator. Moreover, the proposed ASTSMC does not need to obtain the bound of uncertainties in advance and ensures that the sliding variable and its derivative reach to zero in a finite time. In addition, the stability of the closed-loop is proved by Lyapunov theory. Simulation and experiment results demonstrate that the proposed ASTSMC can effectively mitigate the lumped uncertainties and obviously improve the tracking performance.

Keywords: hydraulic servo actuator, nonlinear features, modeling uncertainties, super-twisting sliding mode control

Highlights

- The dynamic mathematical model of hydraulic servo actuator is established considering nonlinear features and modeling uncertainties.
- The ESO is used to estimate the unmeasured system state and lumped uncertainties.
- The ASTSMC is adopted to compensate the disturbance and further improve the tracking precision.
- The simulation and experiment results validate the effectiveness of the ASTSMC based on ESO.

0 INTRODUCTION

Hydraulic servo actuator is widely employed in modern industrial, such as heavy vehicle [1] and [2], load simulator [3], hot-pressing equipment [4], hydraulic manipulator [5], due to the virtues of small size-to-power ratio, high control precision, fast response performance and strong bearing capacity [6] to [8]. However, the nonlinear features and modeling uncertainties of hydraulic servo actuator complicates the dynamic model and hinders position tracking performance. The nonlinear features are mainly caused by pressure-flow characteristic of servo valve and nonlinear friction of hydraulic actuator [9] to [12]. While the modeling uncertainties are mostly caused by time-varying hydraulic parameters, unmodeled friction and external disturbance [13] to [15]. Hence, the traditional linear control schemes have become more and more difficult to satisfy the high precision position tracking control requirement of modern hydraulic servo actuator. Importantly, it is essential to study high performance control strategy for hydraulic servo actuator.

In recent years, numerous control schemes have been proposed, such as adaptive control [16], robust control [17], backstepping control [18], sliding mode

control (SMC) [19], and intelligent control [20] to improve the control performance of hydraulic servo system. As an effective control method, SMC can cope with uncertainties and achieve asymptotic tracking performance [21] to [23]. However, the inevitable chattering of SMC caused by discontinuous control input is not acceptable for practical systems. To solve this problem, the continuous switching function, such as continuous saturation function and hyperbolic function, is used to replace the discontinuous symbol function in conventional SMC. Although the tracking error of improved control scheme is bounded, it loses the asymptotic tracking performance. The high order sliding mode controller can ensure the continuity of SMC and obtain the asymptotic tracking performance. However, it needs the derivative information of the sliding mode variable, which is often unattainable in practice, so it is difficult to be realized in engineering practice. In hydraulic servo system, only parts of states can be measured, and load or disturbance cannot be measured directly. Hence, an ESO is used to estimate the immeasurable system state variables and lumped uncertainties in this paper [24]. The proposed ASTSMC can effectively avoid the above drawbacks, but the controller gain related to the upper bound of modeling uncertainty needs to be

*Corr. Author's Address: School of Mechanical and Electrical Engineering, Henan University of Technology, Zhengzhou, 450001, China, wanzhenshuai@haut.edu.cn

set artificially, which is conservative to some extent. The feedforward adaptive control law based on model is introduced into the ASTSMC to improve the control precision of actuator. Moreover, the proposed method does not need to know the exact bound of modeling uncertainty, rather designs an adaptive law to constantly adjust the controller gain associated with the bound. In particular, ASTSMC can make the tracking error converge asymptotically to a small adjustable range near zero in finite time.

The rest of this paper is organized as follows. Section 1 gives system description and dynamical model. The ASTSMC design process and theoretical result are presented in section 2. Simulation results and discussion are depicted in section 3. Section 4 carries experimental setup and comparative results. Finally, the conclusions are summarized in section 5.

1 SYSTEM DESCRIPTION AND DYNAMICAL MODEL

The schematic diagram of the hydraulic servo actuator is given in Fig. 1, which mainly includes pump, motor, servo valve and hydraulic actuator.

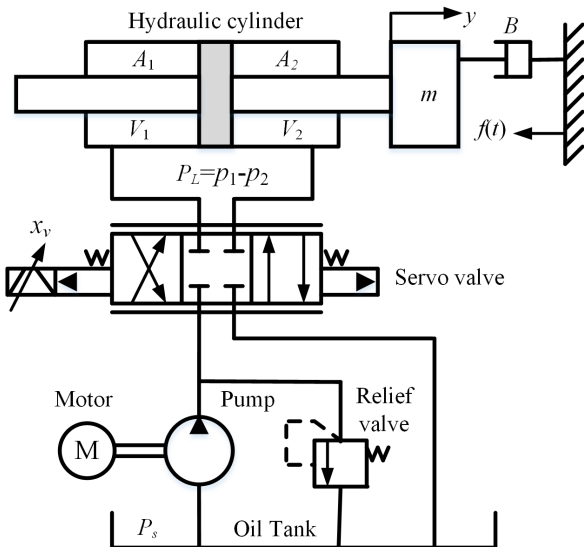


Fig. 1. Schematic diagram of the hydraulic servo actuator

The system mainly consists of three subsystems which are the servo system, the hydraulic part and the mechanical section. The hydraulic part supplies energy for overall equipment. The servo system provides the hydraulic pressure to the mechanical section by controlling the piston's movement. As an executive part, the performance of actuator directly influences the precision of hydraulic driven system. However, many hydraulic servo actuator models have

not adequately account for the impact of nonlinear features and modeling uncertainties. To improve the position control performance of the hydraulic servo actuator, the dynamic model considering various disturbance and uncertainties is used to replace the traditional linear model.

According to the Newton's second law, the dynamic equation of load can be described as

$$m\ddot{y} = P_L A - B\dot{y} - f(t), \quad (1)$$

where m is the equivalent load mass, y is the load displacement, P_L is the load pressure, A is of effective piston area of hydraulic cylinder, B is viscous friction coefficient, $f(t)$ is the nonlinear features and modeling uncertainties.

Ignoring external leakage of hydraulic cylinder, the dynamic equation of load pressure can be written as

$$\frac{V_t}{4\beta_e} \dot{P}_L = Q_L - A\dot{y} - C_t P_L + q(t), \quad (2)$$

where V_t is total volume of hydraulic actuator, β_e is the effective bulk modulus of the hydraulic fluid, Q_L is load flow, C_t is the internal leakage coefficient of hydraulic cylinder, $q(t)$ is the disturbance.

The load flow of servo valve can be constructed as

$$Q_L = k_t u \sqrt{P_s - \text{sign}(u) P_L}, \quad (3)$$

where k_t is the flow gain coefficient, u is the input control voltage of the servo valve, P_s is the supply pressure of the pump, $\text{sign}(u)$ is defined as

$$\text{sign}(u) = \begin{cases} 1, & \text{if } u \geq 0 \\ -1, & \text{if } u < 0 \end{cases}. \quad (4)$$

For the ease of calculation, let the system states be defined as

$$x = [x_1, x_2, x_3]^T = [y, \dot{y}, \ddot{y}]^T. \quad (5)$$

Combing Eqs. (1) to (5), the state space model of the hydraulic servo actuator is given by

$$\begin{cases} \dot{x}_1 = x_2 \\ \dot{x}_2 = x_3 \\ \dot{x}_3 = f_1(u, P_L)u - f_2(x_2) - f_3(x_3) + d(t) \end{cases}, \quad (6)$$

where

$$\begin{cases} f_1(t) = \frac{4\beta_e Ak_t}{mV_t} \sqrt{P_s - \text{sign}(u)P_L} \\ f_2(t) = \frac{4\beta_e}{mV_t} (A^2 + BC_t) x_2 \\ f_3(t) = \frac{4\beta_e}{mV_t} \left(C_t m + \frac{BV_t}{4\beta_e} \right) x_3 \\ d(t) = \frac{4\beta_e A}{mV_t} q(t) - \frac{4\beta_e C_t}{mV_t} f(t) - \frac{\dot{f}(t)}{m} \end{cases}$$

The greatest difficulties in this model is the high nonlinearity with respect the control signal and unmodeled disturbance for hydraulic servo actuator. To cope with this problem, the ASTSMC is utilized to drive the load track the desired trajectory as closely as possible.

2 CONTROLLER DESIGN

2.1 Extended State Observer

Set the lumped uncertainties of $d(t)$ as an extended state x_4 , then Eq. (6) can be rewritten as

$$\begin{cases} \dot{x}_1 = x_2 \\ \dot{x}_2 = x_3 \\ \dot{x}_3 = f_1(u, P_L)u - f_2(x_2) - f_3(x_3) + x_4 \\ \dot{x}_4 = \dot{d}(t) \end{cases} \quad (7)$$

Note that $q(t)$ and $f(t)$ are bounded, thus $d(t)$ is bounded by a known positive constant δ .

Design an ESO of the Eq. (7) as

$$\begin{cases} \hat{x}_1 = \hat{x}_2 - \beta_1 (\hat{x}_1 - x_1) \\ \hat{x}_2 = \hat{x}_3 - \beta_2 (\hat{x}_1 - x_1) \\ \hat{x}_3 = \hat{f}_1(u, P_L)u - \hat{f}_2(x_2) - \hat{f}_3(x_3) + \hat{x}_4 - \beta_3 (\hat{x}_1 - x_1) \\ \hat{x}_4 = -\beta_4 (\hat{x}_1 - x_1) \end{cases} \quad (8)$$

where \hat{x}_i is the estimation states of the ESO, \hat{f}_i is the estimations of f_i , β_i is the observe gains to be determined.

Define $\varepsilon_i = x_i - \hat{x}_i$, the dynamic of error is

$$\begin{aligned} \dot{\varepsilon} &= A\varepsilon - L(\hat{x}_1 - x_1) + B_w d + F \\ &= (A - LC)\varepsilon + B_w d + F, \end{aligned} \quad (9)$$

where \tilde{f}_i is the estimation error of f_i , and

$$A = \begin{bmatrix} 0 & 1 & 0 & 0 \\ 0 & 0 & 1 & 0 \\ 0 & 0 & 0 & 1 \\ 0 & 0 & 0 & 0 \end{bmatrix}, \quad L = \begin{bmatrix} \beta_1 \\ \beta_2 \\ \beta_3 \\ \beta_4 \end{bmatrix}, \quad C = \begin{bmatrix} 1 \\ 0 \\ 0 \\ 0 \end{bmatrix}^T, \quad B_w = \begin{bmatrix} 0 \\ 0 \\ 0 \\ 1 \end{bmatrix},$$

$$F = \begin{bmatrix} 0 \\ 0 \\ \tilde{f}_1 u - \tilde{f}_2 - \tilde{f}_3 \\ 0 \end{bmatrix}.$$

To ensure the pole of matrix $(A - LC)$ on the left half plane, the characteristic polynomial can be written as

$$\lambda_0(s) = [sI - (A - LC)] = (s + w_0)^4, \quad (10)$$

where w_0 is the bandwidth of the observe.

The parameters of ESO are selected as

$$\beta_1 = 4w_0, \beta_2 = -6w_0^2, \beta_3 = 4w_0^3, \beta_4 = -4w_0^4. \quad (11)$$

Assumption 1: The unmodeled disturbances are bounded and satisfy

$$d(t) \leq M_1, |\dot{d}(t)| \leq M_2, |F(t)| \leq M_3, \quad (12)$$

where M_1, M_2, M_3 are unknown positive constants.

Theorem 1: The estimated error of the ESO can be expressed as

$$\lim_{t \rightarrow \infty} \varepsilon(t) = 0. \quad (13)$$

Proof: Define $A_1 = A - LC$, then

$$\begin{aligned} \varepsilon(t) &= \exp(A_1 t) \varepsilon(0) + \int_0^t \exp((A_1(t - \tau)) F d \tau \\ &\quad + \int_0^t \exp((A_1(t - \tau)) B_w d(t) d \tau. \end{aligned} \quad (14)$$

Using the property of matrix norms, Eq. (14) can be represented as

$$\begin{aligned} \|\varepsilon(t)\| &\leq \|\exp(A_1 t)\| \|\varepsilon(0)\| \\ &\quad + \int_0^t \|\exp((A_1(t - \tau))\| \|B_w\| \|d(t)\| d \tau \\ &\quad + \int_0^t \|\exp((A_1(t - \tau))\| \|F\| d \tau. \end{aligned} \quad (15)$$

Based on Eq. (10), the eigenvalues of A_1 are $\lambda_1 = \lambda_2 = \lambda_3 = -w_0$, then there exists $\kappa > 1$ such that for all $t \geq 0$

$$\begin{cases} \|\exp(A_1 t)\| \leq \kappa \exp(-w_0 t) \\ \|\exp((A_1(t - \tau))\| \leq \kappa \exp(-w_0(t - \tau)) \end{cases} \quad (16)$$

Then the Eq. (15) can be represented as

$$\|\varepsilon(t)\| \leq \kappa \|\exp(-w_0 t)\| \|\varepsilon(0)\| + \frac{\kappa M_1}{w_0} (1 - \exp(-w_0 t)) + \frac{\kappa M_3}{w_0} (1 - \exp(-w_0 t)). \quad (17)$$

Therefore, if the w_0 goes to infinity, the $\varepsilon(t)$ would be convergent to zero.

2.2 Adaptive Super-twisting Sliding Mode Controller

The tracking errors are defined as

$$\begin{cases} z_1 = x_1 - x_{1d} \\ z_2 = x_2 - \dot{x}_{1d} \\ z_3 = x_3 - \ddot{x}_{1d} \end{cases}, \quad (18)$$

where z_1, z_2, z_3 are tracking error of position, velocity and acceleration, respectively.

The sliding mode surface is defined as

$$s = k_1 z_1 + k_2 z_2 + z_3, \quad (19)$$

where k_1 and k_2 are positive constants.

The derivative of s can be written as

$$\begin{aligned} \dot{s} &= k_1 z_2 + k_2 z_3 + \dot{z}_3 \\ &= k_1 z_2 + k_2 z_3 + f_1(u, P_L)u - f_2(x_2) - f_3(x_3) - \ddot{x}_{1d}. \end{aligned} \quad (20)$$

The control input of super-twisting sliding mode controller is designed as

$$u = \frac{1}{f_1(u, P_L)} \left\{ \underbrace{\left[\frac{f_2(x_2) + f_3(x_3) + \ddot{x}_{1d}}{u_1} - k_1 z_1 - k_2 z_3 - \alpha |s|^{1/2} \text{sign}(s) \right]}_{u_2}, \quad (21)$$

where u_1 and u_2 are feedforward control law and robust control law, α and θ are time varying controller gains.

The adaptive laws are defined as

$$\begin{cases} \dot{\alpha} = \gamma_1 \sqrt{\omega} / 2 \text{sign}(|s| - v) \\ \dot{\theta} = 2\varepsilon\alpha \end{cases}, \quad (22)$$

where $\gamma_1, \omega, \theta, v$ are positive constants.

According to Eqs. (21) and (22), the dynamics of s are represented as

$$\begin{cases} \dot{s} = -\alpha |s|^{1/2} \text{sign}(s) + \eta + d(t) \\ \dot{\eta} = -\frac{\theta}{2} \text{sign}(s) \end{cases}. \quad (23)$$

Define state vector $\xi = [\xi_1, \xi_2]^T = [|s|^{1/2} \text{sign}(s), \eta]^T$, then the unmodeled uncertainties are expressed as

$$d(t) = \rho(x, t) |s|^{1/2} \text{sign}(s) = \rho(x, t) \xi_1, \quad (24)$$

where $\rho(x, t)$ is a positive function.

Then, the new state equation is defined as

$$\dot{\xi} = A\xi, \quad (25)$$

where $A = \frac{1}{2|\xi_1|} \begin{bmatrix} \rho(x, t) - \alpha & 1 \\ -\theta & 0 \end{bmatrix}$.

A Lyapunov function is represented as

$$V = V_0 + \frac{1}{2\psi_1} (\alpha - \alpha_0)^2 + \frac{1}{2\psi_2} (\theta - \theta_0)^2, \quad (26)$$

where α_0 and θ_0 are positive constants. V_0 is defined as follows

$$V_0 = \xi^T P \xi, \quad (27)$$

where $P = \begin{bmatrix} \lambda + 4\varepsilon^2 & 2\varepsilon \\ -2\varepsilon & 1 \end{bmatrix}$, λ is a positive constant.

The derivative of V_0 is written as

$$\begin{aligned} \dot{V}_0 &= \dot{\xi}^T P \xi + \xi^T P \dot{\xi} = \xi^T (A^T P + P A) \xi \\ &= -\frac{1}{2|\xi_1|} \xi^T A \xi, \end{aligned} \quad (28)$$

where

$$\begin{aligned} A &= \begin{bmatrix} A_{11} & A_{12} \\ A_{21} & A_{22} \end{bmatrix}, A_{11} = -2(\lambda + 4\varepsilon^2)(\rho - \alpha) - 4\varepsilon\theta, \\ A_{12} &= 2\varepsilon(\rho - \alpha) + \theta - \lambda - 4\varepsilon^2, \\ A_{21} &= 2\varepsilon(\rho - \alpha) + \theta - \lambda - 4\varepsilon^2, A_{22} = 4\varepsilon. \end{aligned}$$

When α satisfies

$$\alpha > \frac{\delta(\lambda + 4\varepsilon^2) - \varepsilon}{\lambda(1 - \psi_1)} + \frac{(2\varepsilon\delta - \lambda - 4\varepsilon^2)^2}{12\varepsilon\lambda(1 - \psi_1)}. \quad (29)$$

We have

$$V_0 \leq -\frac{\varepsilon}{|\xi_1|} \xi^T \xi = -\frac{\varepsilon}{|\xi_1|} \|\xi\|. \quad (30)$$

According to the following inequalities

$$\begin{cases} \lambda_{\min}(P) \|\xi\|^2 \leq \xi^T P \xi \leq \lambda_{\max}(P) \|\xi\|^2 \\ |\xi_1| = |s|^{1/2} \leq \|\xi\| \leq \frac{V_0^{1/2}}{\lambda_{\min}^{1/2}(P)} \end{cases}, \quad (31)$$

where $\lambda_{\max}(P)$ and $\lambda_{\min}(P)$ are maximum and minimum eigenvalue of matrix P , respectively.

Thus, Eq. (31) can be rewritten as

$$\dot{V}_0 \leq -\zeta V_0^{1/2}, \quad (32)$$

where $\zeta = \varepsilon \lambda_{\min}^{1/2}(\mathbf{P}) / \lambda_{\max}(\mathbf{P})$.

Then, the time derivative can be given as

$$\begin{aligned} \dot{V} &= \dot{V}_0 + \frac{1}{\psi_1}(\alpha - \alpha_0)\dot{\alpha} + \frac{1}{\psi_2}(\theta - \theta_0)\dot{\theta} \\ &\leq -\sigma V_0^{1/2} \frac{1}{\psi_1}(\alpha - \alpha_0)\dot{\alpha} + \frac{1}{\psi_2}(\theta - \theta_0)\dot{\theta} \\ &\quad + \frac{\gamma_1}{\sqrt{2\psi_1}}|\alpha - \alpha_0| + \frac{\gamma_2}{\sqrt{2\psi_2}}|\theta - \theta_0|, \end{aligned} \quad (33)$$

where $\sigma = \min\{\zeta, \gamma_1, \gamma_2\}$.

$$\begin{aligned} \dot{V} &\leq -\sigma V_0^{1/2} + \frac{1}{\psi_1}(\alpha - \alpha_0)\dot{\alpha} + \frac{1}{\psi_2}(\theta - \theta_0)\dot{\theta} \\ &\quad + \frac{\gamma_1}{\sqrt{2\psi_1}}|\alpha - \alpha_0| + \frac{\gamma_2}{\sqrt{2\psi_2}}|\theta - \theta_0|. \end{aligned} \quad (34)$$

Based on Eq. (22), there exists positive constants α_0 and β_0 , which satisfy $\alpha - \alpha_0 < 0$ and $\beta - \beta_0 < 0$. Then Eq. (33) can be represented as

$$\begin{cases} \dot{\alpha} = \gamma_1 \sqrt{\psi_1/2}, \dot{\theta} = \gamma_2 \sqrt{\psi_2/2} & |s| > v \\ \dot{\alpha} = -\gamma_1 \sqrt{\psi_1/2}, \dot{\theta} = -\gamma_2 \sqrt{\psi_2/2} & |s| < v \end{cases}, \quad (35)$$

Assuming $v=0$, we know that $s \rightarrow 0$ in finite time, and

$$t_f \leq \frac{2V^{1/2}(t_0)}{\sigma}. \quad (36)$$

3 SIMULATION RESULTS

To show the trajectory tracking performance of the presented ASTSMC, PID and SMC schemes are first utilized for simulation comparison. It should be noted that all controller parameters are set through a preliminary tuning process. The parameters of hydraulic servo actuator are listed in table 1.

- 1) PID: The gains of PID controller are tuned as $K_p=120$, $K_i=10$, $K_d=0.1$ to balance the steady-state error and transient response performance.
- 2) SMC: Based on SMC scheme, the control law is designed as

$$u = \frac{1}{f_1(u, P_L)} \left\{ \begin{aligned} &f_2(x_2) + f_3(x_3) + \ddot{x}_{1d} \\ &-k_1 z_1 - k_2 z_3 - k_3 \text{sign}(s) \end{aligned} \right\}, \quad (37)$$

where $k_1 = 4 \times 10^3$, $k_2 = 2 \times 10^3$, $k_3 = 2 \times 10^2$.

- 3) ASTSMC: The parameters of proposed ASTSMC are given as $k_1 = 2 \times 10^3$, $k_2 = 6 \times 10^2$, $k_3 = 2 \times 10^2$, $\gamma_1 = 2$, $\omega = 6$, $\theta = 5$, $v = 2$. Note that the sign function in Eq. (21) is replaced with saturation

function for meeting the requirement of the control input continuous.

Table 1. The parameters of hydraulic servo actuator

Parameter	Value
m	300 kg
V_t	$9 \times 10^{-5} \text{ m}^3$
ρ	900 kg/m ³
B	1200 N-s/m
C_t	4×10^{-3}
β_e	$6.9 \times 10^8 \text{ Pa}$
K_t	$7.2 \times 10^{-7} \text{ m/V}$
A	$3.14 \times 10^{-4} \text{ m}^2$

To validate the advantages of the proposed ASTSMC, a sinusoidal signal $x_d = 60 \sin(20\pi t)$ mm is used as reference trajectory. The position tracking performance and tracking error are given in Figs. 2 and 3, from which we can see that the proposed ASTSMC is better than the SMC and PID. This is because the proposed ASTSMC can estimate the unknown dynamics by ESO and compensate that by adaptive control law. Compared with the PID controller, the tracking errors of SMC and ASTSMC are substantially reduced by 18.3 % and 48.8 %, respectively. Fig. 4 shows the control input of the three controllers. It is noted that owing to the adaptive mechanism in ASTSMC, its control input is smaller than PID and SMC. The observation performance of ESO to external interference is shown in Fig. 5. It is clearly indicated that the ESO can estimate the state variavbe and lumped uncertainties accurately.

In order to further authenticate the rationality of ASTMC, multi-frequency sinusoidal signal $x_d = 50 \sin(10\pi t) + 40 \sin(25\pi t) + 20 \sin(50\pi t)$ [mm] is selected as reference signal. Also, the simulation results are shown in Figs. 6 and 7. It is noted that three controllers can track the reference trajectory accurately. However, the proposed ASTSMC obtains the smallest tracking error than SMC and PID, which verifies the superiority of the proposed controller. The maximum tracking errors of PID, SMC and ASTSM are 20.471 mm, 14.237 mm, 8.690 mm, respectively.

In order to quantitatively compare the tracking performance of different controllers, maximum absolute value of tracking error M_e , average tracking error μ_e , and standard deviation of tracking error σ_e are adopted as performance indices. Table 2 summarizes the performance indices of different controllers for sinusoidal and multi-frequency sinusoidal motion reference signal. It can be found that the proposed ASTSMC produces the smallest values among three

controllers. In addition, the performance indices of SMC are better than PID. The simulation results clearly demonstrate that the proposed ASTSM can

provide a better control performance for the hydraulic servo actuator with unknown dynamics than the others under different reference trajectories.

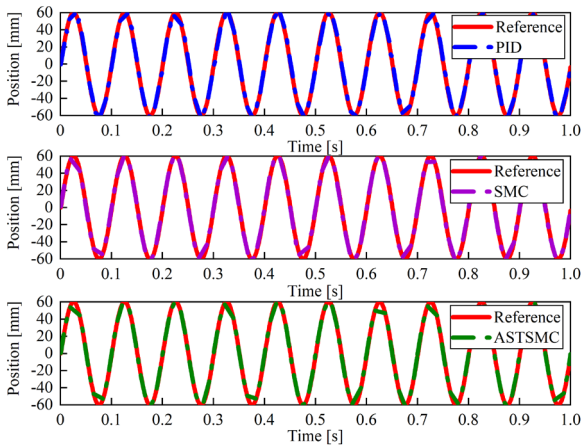


Fig. 2. Position tracking of sinusoidal motion

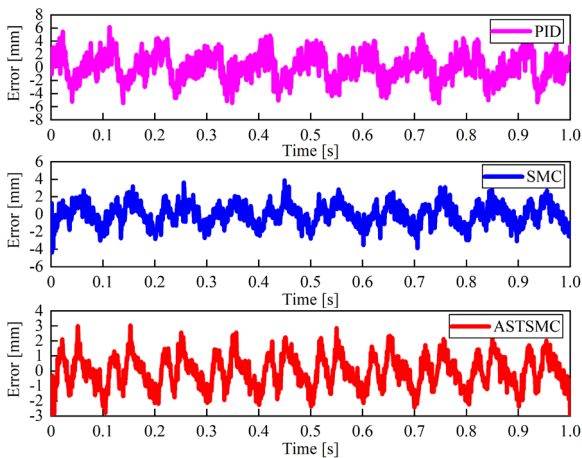


Fig. 3. Tracking error of sinusoidal motion

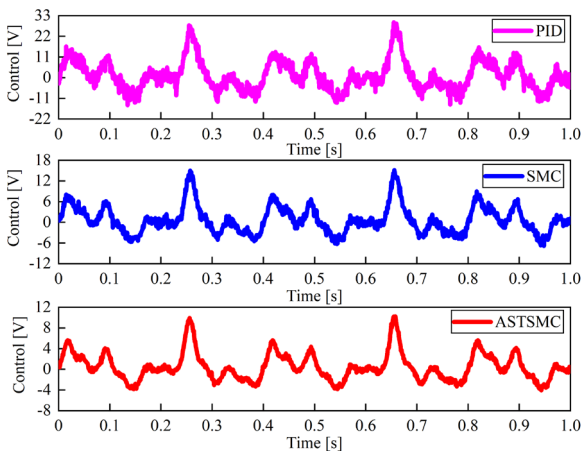


Fig. 4. Control law of sinusoidal motion

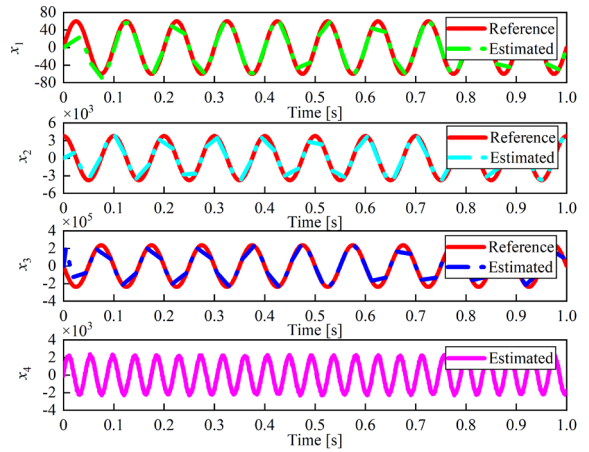


Fig. 5. The observation performance of ESO

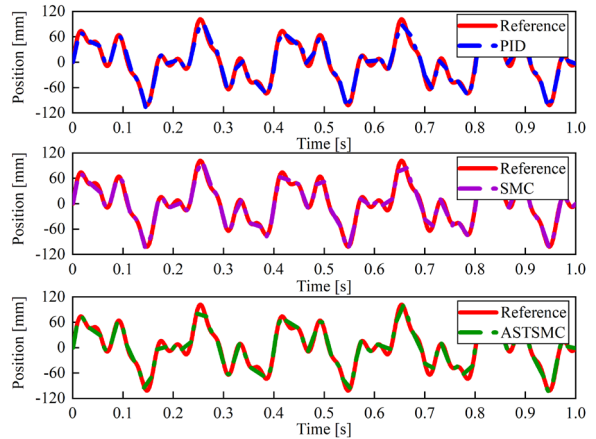


Fig. 6. Position tracking of multi-frequency sinusoidal motion

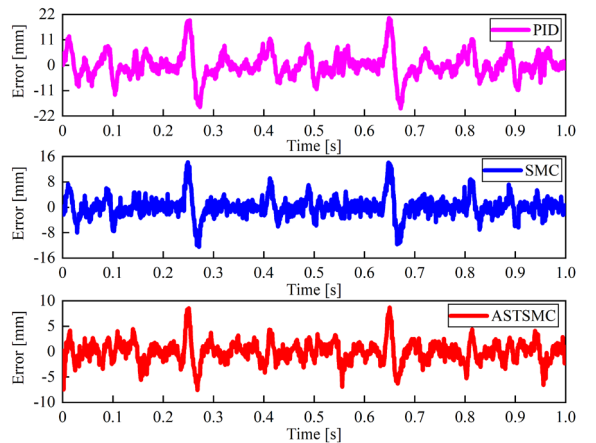


Fig. 7. Tracking error of multi-frequency sinusoidal motion

Table 2. Comparison results of performance indices

Signal	Controller	M_e	μ_e	σ_e
Sinusoidal	PID	6.147	1.682	1.225
	SMC	5.023	1.459	1.111
	ASTSMC	3.145	0.881	0.595
Multi-frequency sinusoidal	PID	20.471	3.909	3.825
	SMC	14.237	2.267	2.463
	ASTSMC	8.690	1.556	1.435

4 EXPERIMENTAL RESULTS

In this section, a hydraulic servo actuator experimental setup is used to demonstrate the effectiveness of the proposed control scheme. The diagram of experimental setup is shown in Fig 8. The host computer offers human-computer interaction interface for compiling programs and adjusting controller parameters. The Target computer reads the feedback signal real time and feeds it back to the host computer by TCP/IP protocol. The digital control signal is converted to analogue signal by D/A card and processed by signal conditioner, and then sent to the servo valve to drive the hydraulic servo actuator. The position and pressure information are collected by position sensor and pressure sensor, respectively. The A/D card obtains the sensors information and sends them to target computer to form closed-loop control system by signal conditioner.

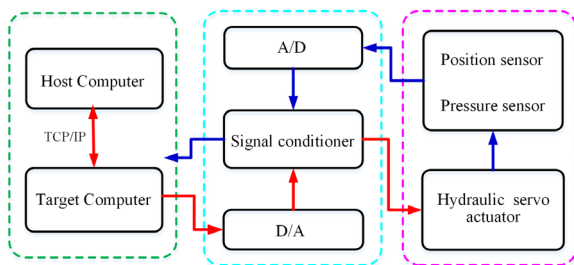


Fig. 8. The diagram of experimental setup

The load is first commanded to track a low-speed motion $x_d=40\sin(10\pi t)$ [mm]. The obtained position tracking and tracking error are displayed in Figs. 9 and 10. It can be seen that the proposed controller ASTSMC delivers smaller tracking error than PID and SMC, because they use ESO to estimate the lumped uncertainties. In addition, the tracking error of all controllers occurs chattering when the trajectory is reversed due to the unmodeled dynamic characteristic and measurement noise. However, the chattering value of the proposed ASTSMC is smaller to other controllers, which means that the control

scheme based ESO and adaptive law is very helpful to alleviate the effects from lumped uncertainties in hydraulic system.

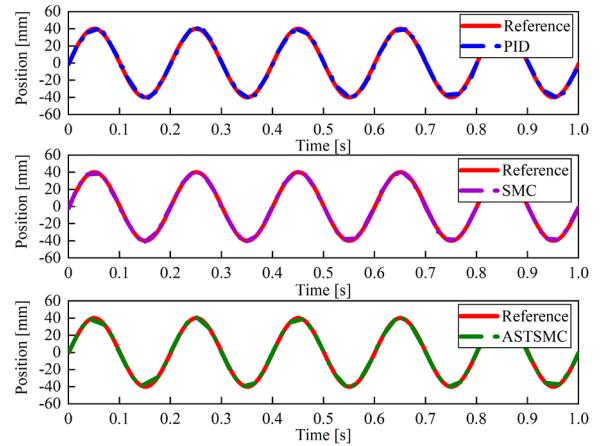


Fig. 9. Position tracking of $x_d=40\sin(10\pi t)$ [mm]

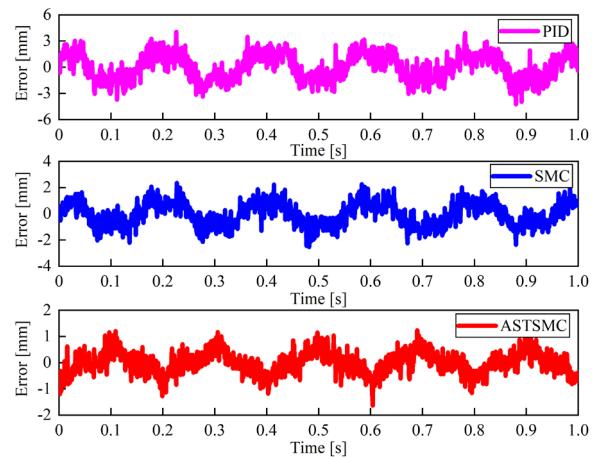


Fig. 10. Tracking error of $x_d=40\sin(10\pi t)$ [mm]

To further verify the superiority of the ASTMC, a high-speed motion $x_d = 40\sin(15\pi t)$ is performed as reference signal. The experimental comparison results of three controllers are exhibited in Figs. 11 and 12. As presented, the proposed ASTSMC attains better tracking precision in comparison to the other controllers. This is because that the control gains in ASTSMC can dynamically be adjusted as unknown uncertainties changes.

In this case, a large amplitude motion signal $x_d = 80\sin(15\pi t)$ mm is chose as the reference trajectory with the amplitude of 80 mm and the frequency 7.5 Hz. The corresponding position tracking performance and tracking error are presented in Figs. 13 and 14. It is noted that the three controllers are all able to suppress the nonlinear features and modeling

uncertainties for such a large amplitude tracking test. However, the proposed ASTSMC shows excellent tracking performance than the other two compared

controllers. The tracking error of ASTSMC is always within in 8 mm, showing a good tracking precision.

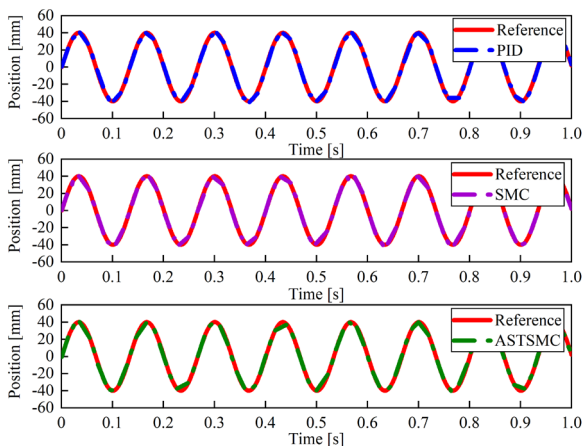


Fig. 11. Position tracking of $x_d = 40\sin(15\pi t)$ [mm]

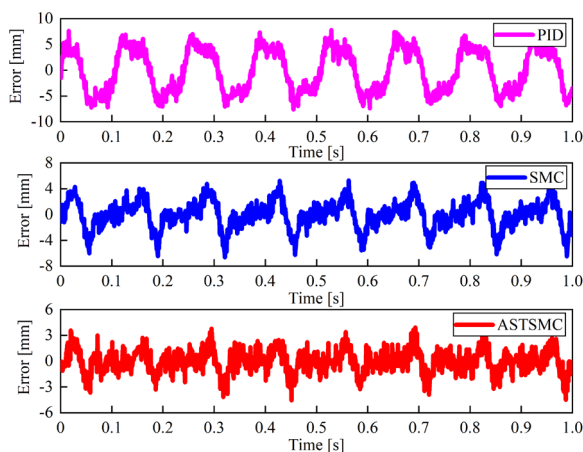


Fig. 14. Tracking error of $x_d = 80\sin(15\pi t)$ [mm]

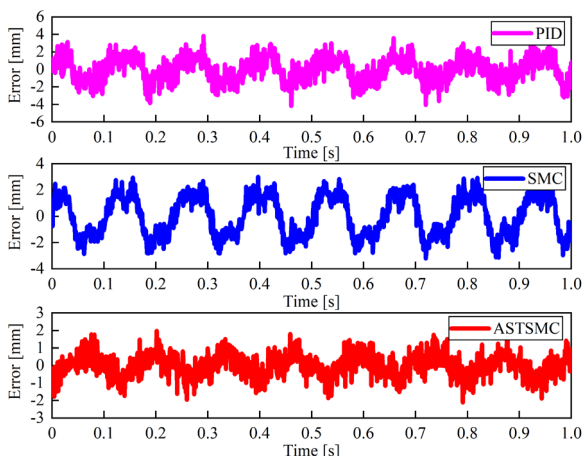


Fig. 12. Tracking error of $x_d = 40\sin(15\pi t)$ [mm]

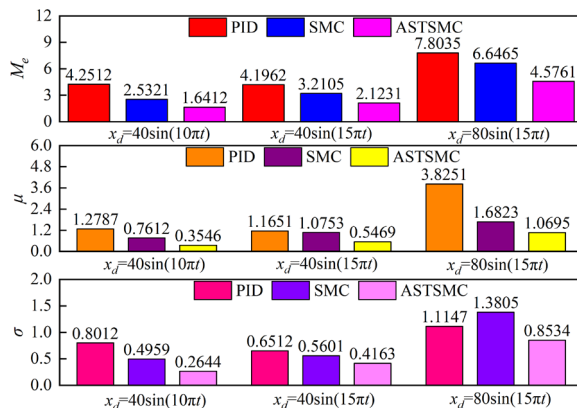


Fig. 15. Comparison performance indices of controllers

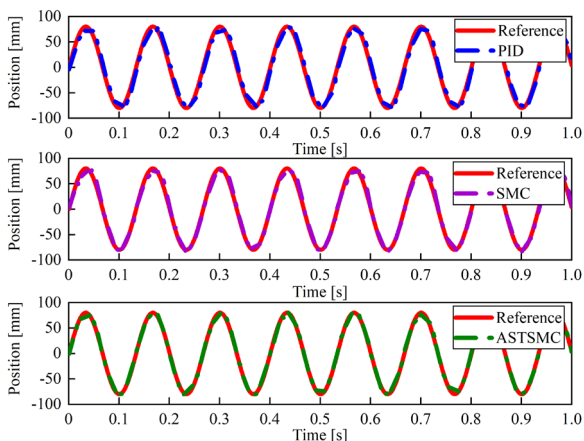


Fig. 13. Position tracking of $x_d = 80\sin(15\pi t)$ [mm]

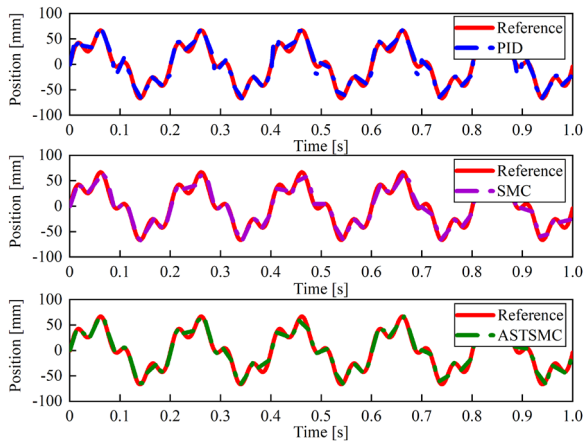


Fig. 16. Position tracking of $x_d = 50\sin(10\pi t) + 20\sin(40\pi t)$ [mm]

The performance indices of three controllers for different sinusoidal motion are shown in Fig. 15. One can find that the values of performance indices with the ASTSMC are the smallest among all controllers. The maximum errors of above experimental situation are 1.6412 mm and 2.1231 mm for amplitude 40 mm, respectively. In particular, the maximum of relative average error of ASTSMC is within 1.35 %, which demonstrates the effectiveness of the proposed control scheme.

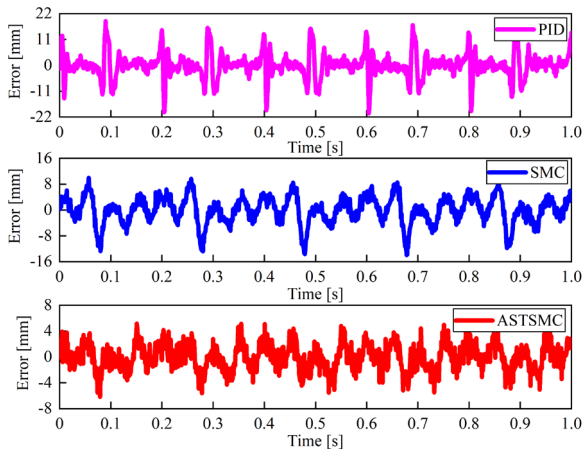


Fig. 17. Tracking error of $x_d = 50\sin(10\pi t) + 20\sin(40\pi t)$ [mm]

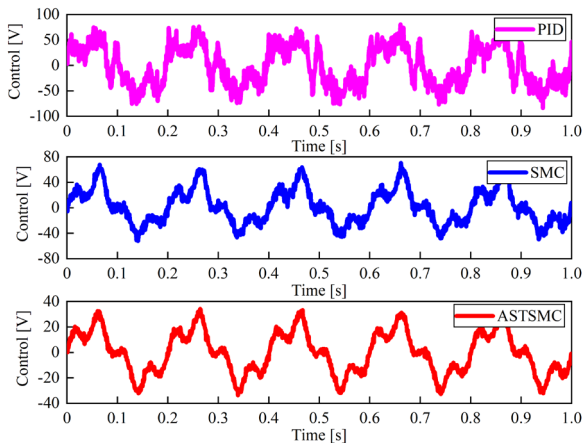


Fig. 18. Control law of $x_d = 50\sin(10\pi t) + 20\sin(40\pi t)$ [mm]

Multi-frequency sinusoidal experimental results $x_d = 50\sin(10\pi t) + 20\sin(40\pi t)$ are shown in Figs. 16 and 17. It can be seen that the presented controller ASTSMC can track the reference signal accurately, and the tracking error is smaller than SMC and PID. Especially, PID controller gives the worst control performance. It is evident that the tracking error of ASTSMC is within 5 mm, and that of PID, SMC is within 22 mm and 15 mm, respectively, which proves the high-accuracy tracking performance of the

designed control scheme again. The control inputs of different controllers are shown in Fig 18. As shown, although the input of all controller is bounded, the input of ASTSMC is smaller than PID and SMC.

5 CONCLUSIONS

In this paper, a ASTSMC scheme based on ESO has been proposed for hydraulic servo actuator with nonlinear features and modeling uncertainties. First, the dynamical mathematical model containing various nonlinear and uncertainties is established. The parameter adaptive law is used to update the controller gain in real time to avoid the conservativeness caused by artificial setting. The obtained control input is continuous, which avoids the chatter problem of traditional sliding mode controller. The stability analysis demonstrates that the tracking error of the system converges asymptotically to an arbitrarily small range near zero in finite time, and the convergence rate and the bounds of steady-state error can be adjusted by parameters. Extensive comparative simulation and experimental results show that the proposed ASTSMC can make the position trajectory track the reference command well and satisfy the high precision control of the servo system.

6 ACKNOWLEDGEMENTS

This work is supported by the Key Science and Technology Program of Henan Province (222102220104) and the High-Level Talent Foundation of Henan University of Technology (2020BS043).

7 REFERENCES

- [1] Hu, C.A., Gao, H.B., Guo, J.H., Taghavifar, H., Qin, Y.C., Na, J., Wei, C. F. (2021). RISE-based Integrated Motion Control of autonomous ground vehicles with asymptotic prescribed performance. *IEEE Transactions on Systems Man Cybernetics-Systems*, vol. 51, no. 9, p. 5336-5348, DOI:10.1109/tsmc.2019.2950468.
- [2] Huang, Y.B., Na, J., Wu, X., Gao, G.B. (2018). Approximation-Free Control for Vehicle Active suspensions with hydraulic actuator. *IEEE Transactions on Industrial Electronics*, vol. 65, no. 9, p. 7258-7267, DOI:10.1109/tie.2018.2798564.
- [3] Tang, Y., Zhu, Z.C., Shen, G., Rui, G.C., Cheng, D., Li, X., Sa, Y.J., (2019). Real-time nonlinear adaptive force tracking control strategy for electrohydraulic systems with suppression of external vibration disturbance. *Journal of the Brazilian Society of Mechanical Sciences and Engineering*, vol. 41, p. 1-16, DOI:10.1007/s40430-019-1780-1.

- [4] Zhu, L.K., Wang, Z.B., Qiang, H., Liu, Y.Q. (2019). Global sliding-mode dynamic surface control for MDF continuous hot-pressing slab thickness via LESO. *International Journal of Machine Learning and Cybernetics*, vol. 10, p. 1249-1258, DOI:10.1007/s13042-018-0804-y.
- [5] Guo, Q., Chen, Z.L. (2021). Neural adaptive control of single-rod electrohydraulic system with lumped uncertainty. *Mechanical Systems and Signal Processing*, vol. 146, p. 1-17, DOI:10.1016/j.ymssp.2020.106869.
- [6] Guo, Q., Chen, Z. L., Shi, Y., Liu, G. (2021). Model identification and parametric adaptive control of hydraulic manipulator with neighborhood field optimization. *IET Control Theory and Applications*, vol. 15, no. 12, p. 1599-1614, DOI:10.1049/cth2.12145.
- [7] Yang, X.W., Deng, W.X., Yao, J.Y. (2022). Neural network based output feedback control for DC motors with asymptotic stability. *Mechanical Systems and Signal Processing*, vol. 164, p. 1-15, DOI:10.1016/j.ymssp.2021.108288.
- [8] Guo, Q., Yin, J. M., Yu, T., Jiang, D. (2017). Saturated adaptive control of an electrohydraulic actuator with parametric uncertainty and load disturbance. *IEEE Transactions on Industrial Electronics*, vol. 64, no. 10, p. 7930-7941, DOI:10.1109/tie.2017.2694352.
- [9] Cheng, C., Liu, S.Y., Wu, H.Z. (2020). Sliding mode observer-based fractional-order proportional-integral-derivative sliding mode control for electro-hydraulic servo systems. *Proceedings of the Institution of Mechanical Engineers Part C-Journal of Mechanical Engineering Science*, vol. 234, no. 10, p. 1887-1898, DOI:10.1177/0954406220903337.
- [10] Yin, X.X., Zhang, W.C., Jiang, Z.S., Pan, L. (2019). Adaptive robust integral sliding mode pitch angle control of an electro-hydraulic servo pitch system for wind turbine. *Mechanical Systems and Signal Processing*, vol. 133, p. 1-15 DOI:10.1016/j.ymssp.2018.09.026.
- [11] Zhao, J.S., Wang, Z.P., Yang, T., Xu, J.X., Ma, Z.L., Wang, C.F. (2020). Design of a novel modal space sliding mode controller for electro-hydraulic driven multi-dimensional force loading parallel mechanism. *ISA Transactions*, vol. 99, p. 374-386, DOI:10.1016/j.isatra.2019.09.018.
- [12] Jing, C.H., Xu, H.G., Jiang, J.H. (2019). Flatness-based adaptive nonlinear control for torque tracking of electro-hydraulic friction load simulator with uncertainties. *Proceedings of the Institution of Mechanical Engineers Part I-Journal of Systems and Control Engineering*, vol. 233, no. 8, p. 1009-1016, DOI:10.1177/0959651818813230.
- [13] Yao, J.Y. (2018). Model-based nonlinear control of hydraulic servo systems: Challenges, developments and perspectives. *Frontiers of Mechanical Engineering*, vol. 13, no. 2, p. 179-210, DOI:10.1080/00207170701390132.
- [14] Won, D., Kim, W., Tomizuka, M. (2017). High-gain-observer-based integral sliding mode control for position tracking of electrohydraulic servo systems. *IEEE-ASME Transactions on Mechatronics*, vol. 22, no. 6, p. 2695-2704, DOI:10.1109/tmech.2017.2764110.
- [15] Kaddissi, C., Kenne, J. P., Saad, M. (2007). Identification and real-time control of an electrohydraulic servo system based on nonlinear backstepping. *IEEE-ASME Transactions on Mechatronics*, vol. 12, no. 1, p. 12-22, DOI:10.1109/tmech.2006.886190.
- [16] Xin, C., Li, Y.-X., Ahn, C.K. (2022). Adaptive neural asymptotic tracking of uncertain non-strict feedback systems with full-state constraints via command filtered technique. *IEEE Transactions on Neural Networks and Learning Systems*, p. 1-6, DOI:10.1109/tnnls.2022.3141091.
- [17] Deng, W.X., Yao, J.Y., Ma, D.W. (2017). Robust adaptive precision motion control of hydraulic actuators with valve dead-zone compensation. *ISA Transactions*, vol. 70, p. 269-278, DOI:10.1016/j.isatra.2017.07.022.
- [18] Guo, Q., Zhang, Y., Celler, B.G., Su, S.W. (2016). Backstepping control of electro-hydraulic system based on extended-state-observer with plant dynamics largely unknown. *IEEE Transactions on Industrial Electronics*, vol. 63, no. 11, p. 6909-6920, DOI:10.1109/tie.2016.2585080.
- [19] Kolsi-Gdoura, E., Feki, M., Derbel, N. (2015). Position control of a hydraulic servo system using sliding mode with an integral and realizable reference compensation. *Control Engineering and Applied Informatics*, vol. 17, no. 1, p. 111-119.
- [20] Liu, Y.J., Zeng, Q., Liu, L., Tong, S.C. (2020). An adaptive neural network controller for active suspension systems with hydraulic actuator. *IEEE Transactions on Systems Man Cybernetics-Systems*, vol. 50, no. 12, p. 5351-5360, DOI:10.1109/tsmc.2018.2875187.
- [21] Hoang, Q.D., Lee, S.G., Dugarjav, B. (2019). Super-twisting observe-based integral sliding mode control for tracking the rapid acceleration of a piston in a hybrid electro-hydraulic and pneumatic system. *Asian Journal of Control*, vol. 21, no. 1, p. 483-498, DOI:10.1002/asjc.1971.
- [22] Shao, K., Zheng, J.C., Huang, K., Wang, H., Man, Z.H., Fu, M.Y., (2020). Finite-time control of a linear motor positioner using adaptive recursive terminal sliding mode. *IEEE Transactions on Industrial Electronics*, vol. 67, no. 8, p. 6659-6668, DOI:10.1109/tie.2019.2937062.
- [23] Van, M., Do, X. P., Mavrovouniotis, M. (2020). Self-tuning fuzzy PID-nonsingular fast terminal sliding mode control for robust fault tolerant control of robot manipulators. *ISA Transactions*, vol. 96, p. 60-68, DOI:10.1016/j.isatra.2019.06.017.
- [24] Palli, G., Strano, S., Terzo, M. (2018). Sliding-mode observers for state and disturbance estimation in electro-hydraulic systems. *Control Engineering Practice*, vol. 74, p. 58-70, DOI:10.1016/j.conengprac.2018.02.007.